ARL-TR-7681 ● MAY 2016

US Army Research Laboratory

Batch Computed Tomography Analysis of Projectiles

by Michael C Golt, Chris M Peitsch, Matthew S Bratcher, and Eric D Warner

NOTICES

Disclaimers

The findings in this report are not to be construed as an official Department of the Army position unless so designated by other authorized documents.

Citation of manufacturer's or trade names does not constitute an official endorsement or approval of the use thereof.

Destroy this report when it is no longer needed. Do not return it to the originator.

ARL-TR-7681 ● MAY 2016

US Army Research Laboratory

Batch Computed Tomography Analysis of Projectiles

by Michael C Golt and Matthew S Bratcher
Weapons and Materials Research Directorate, ARL

Chris M Peitsch
Chesapeake Testing, Belcamp, MD

Eric D Warner
Bowhead Science and Technology, Belcamp, MD

REPORT DOCUMENTATION PAGE

Form Approved
OMB No. 0704-0188

1. REPORT DATE *(DD-MM-YYYY)*	2. REPORT TYPE	3. DATES COVERED (From - To)
May 2016	Final	November 2015–April 2016

4. TITLE AND SUBTITLE
Batch Computed Tomography Analysis of Projectiles

5a. CONTRACT NUMBER

5b. GRANT NUMBER

5c. PROGRAM ELEMENT NUMBER

6. AUTHOR(S)
Michael C Golt, Chris M Peitsch, Matthew S Bratcher, and Eric D Warner

5d. PROJECT NUMBER

5e. TASK NUMBER

5f. WORK UNIT NUMBER

7. PERFORMING ORGANIZATION NAME(S) AND ADDRESS(ES)
US Army Research Laboratory
ATTN: RDRL-WMM-E
Aberdeen Proving Ground, MD 21005-5069

8. PERFORMING ORGANIZATION REPORT NUMBER
ARL-TR-7681

9. SPONSORING/MONITORING AGENCY NAME(S) AND ADDRESS(ES)

10. SPONSOR/MONITOR'S ACRONYM(S)

11. SPONSOR/MONITOR'S REPORT NUMBER(S)

12. DISTRIBUTION/AVAILABILITY STATEMENT
Approved for public release; distribution is unlimited.

13. SUPPLEMENTARY NOTES

14. ABSTRACT
The use of cartridge projectiles in the ballistic evaluation of armor can result in measurement uncertainty if there is variability in their construction. This report details a method that was developed to batch analyze and compare the volumes of (210) BS41 surrogate projectiles that were scanned using X-ray computed tomography. The method described automatically segments and obtains the axial-symmetric radii profiles of components contained within the projectile (outer jacket, inner jacket, core), which can then be used to quantify and compare projectiles to one another numerically using a root-mean-square-error calculation. Projectiles are then grouped together according to the similarity of their components. Also discussed is graphical-cluster analysis of the projectiles, which aids in understanding the source of their variability as well as an approach to use this method's numerical component values to account for projectile variability in the ballistic evaluation of armor.

15. SUBJECT TERMS
computed tomography, CT, BS41, projectiles, ballistic, armor, grouping, clustering

16. SECURITY CLASSIFICATION OF:			17. LIMITATION OF ABSTRACT	18. NUMBER OF PAGES	19a. NAME OF RESPONSIBLE PERSON
a. REPORT	b. ABSTRACT	c. THIS PAGE			Michael C Golt
Unclassified	Unclassified	Unclassified	UU	28	19b. TELEPHONE NUMBER (Include area code) 410-306-0946

Contents

List of Figures

List of Tables

INTENTIONALLY LEFT BLANK.

1. Introduction

The Russian 14.5-mm heavy machine gun is a threat encountered globally. The 14.5-mm BS41* projectile was first fielded in 1941 as an antitank round that contains a tungsten carbide cobalt (WC-Co) core with an incendiary filler that proved to be effective at defeating armor. As such, BS41 projectiles have been employed domestically as experimental penetrators for armor research and development. Specifications for armor (MIL-DTL-46100E) and standards for armor testing (MIL-STD-662F) have requirements for the experimental use of—and penetration resistance to—the BS41 projectile. Because the projectile serves a vital role as part of an armor-validation system, it is important that the variability between projectiles is understood and considered when evaluating armor performance—unaccounted variability increases the measurement uncertainty.

Some variability could be quantified through simple mass measurements, or by comparing external dimensions. However, modern X-ray computed tomography (CT) technology provides a complete view of the inside of projectiles with high-resolution imaging of the various component densities and their relative shapes and locations in space. Currently, surrogate BS41 projectiles are manufactured for the US Army Research Laboratory (ARL) by New Lenox Ordinance under the product code ARL-41000, in which the incendiary powder located above the tungsten core has been replaced with an inert SiO_2 powder filler. As part of an armor ceramic qualification testing campaign, Chesapeake Testing imaged (210) projectiles through CT prior to ballistic testing to analyze potential variability.

Figure 1 shows cross-sectional images obtained through CT scans on 2 BS41 projectiles that illustrate variability that can be identified through this method. In these images the outer steel jacket is shown with a lower density than the WC-Co core that is wrapped in an inner lead jacket. Significant variability is seen when comparing the projectile in Fig. 1a, which has the lead jacket in a lower position, to Fig. 1b, which has the inner lead jacket in a higher position. The shape of the WC-Co core's tip also differs between the 2 projectiles. To account for this variability in the experimental measurement uncertainty of ballistic testing, these differences between projectiles need to be quantified into numerical values. To do this, the geometries and locations of each component must be extracted from the CT images through an image-analysis step. This report details an image-analysis algorithm for the batch processing of CT data, followed by a methodology for comparing and identifying the variability on a set of (210) BS41 projectiles.

* Russian armor-piercing, antitank, incendiary round, developed in the year 1941.

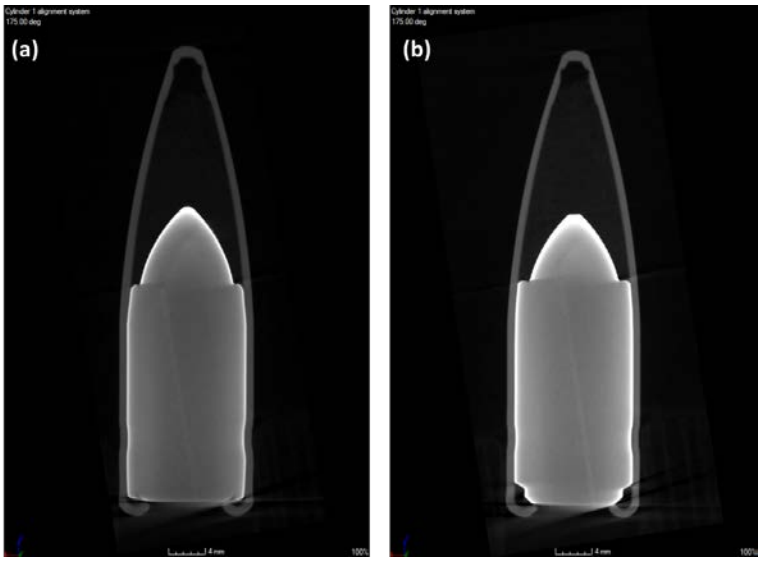

Fig. 1 Profile images obtained from CT scans from 2 BS41 projectiles showing the lead jacket located in 2 different locations: a) lower position, b) higher position

2. Experimental

2.1 CT Scanning at Chesapeake Testing

A group of (210) BS41 projectiles were individually numbered. The projectiles were CT scanned using a Nikon Metrology XT H 320LC cabinet. The X-ray tube energy and current settings were 300 kV and 200 uA, respectively. Each projectile was scanned individually capturing 782 projectile images, a full 360° around the projectile. The samples were imaged at a slight angle to minimize image artifacts along the bottom. Next, a Feldkamp-based reconstruction algorithm was used to generate the raw volumetric file of the projectile. During reconstruction, correction filters were employed to help reduce the effects of beam hardening due to the Pb sleeve and WC-Co core. The resolution of the final volume was 0.068 mm. The volumetric file was then aligned by fitting a cylinder to the outside jacket, and image data was exported in the form of 16-bit ".tiff" files of computed cross-sectional images along the length of the projectile. Given the CT scan and resolution settings, on average 950 computed images were obtained along the length of each projectile to comprise the 3-dimensional (3-D) volume.

With these slices, a reconstructed volume and digital model can be made and subsequent feature segmentation based upon density can be performed as illustrated in Fig. 2.

Fig. 2 Reconstructed and feature segmented volume from ".tiff" stack images. The density of the outer steel jacket is segmented in light blue (semitransparent), the density of the lead jacket and WC-Co core is segmented in orange, and some powder features are visible in dark blue. Projectile ID is 002.

X-rays are able to penetrate through the steel outer jacket as well as the silica filler material in the tip of the projectile. However, the X-rays are nonlinearly absorbed by the lead jacket surrounding the tungsten carbide core (leading to an effect known as beam hardening) and, as such, the core and the jacket cannot be individually segmented and must be analyzed as a single monolithic component. Additional scanning energy could have been used to help with separating the 2 components, but would have resulted in lower resolution.

2.2 CT Image Analysis

An algorithm was developed in Matlab[†] that performed image analysis on each individual cross-sectional image of the projectile. The features of these projectiles are nominally axial symmetric; therefore, their shape, dimensions, and locations in space can be described by the parameters of a circle (i.e., radius, origin). In this manner, a full description of each component (jacket, core, filler area, etc.) can be obtained with a minimum number of descriptor parameters, effectively reducing

[†] Matlab (matrix laboratory) is proprietary commercial software developed by MathWorks.

the amount of information needed to reconstruct the volume. Therefore, the 2-part objective of the CT analysis algorithm was to first segment the images by grayscale intensities corresponding to the densities of the different components, followed by fitting circles to the features in each slice. After obtaining the positions and radii of the circles describing components for each slice along the length of the projectile, other parameters can be calculated such as the steel jacket thickness, the alignment between the core and the outer jacket, and the length of the core tip extending past the inner lead jacket.

2.2.1 Preprocessing and Segmentation

The first objective of the image-analysis algorithm was to segment the cross-sectional slices into the various features of interest according to their densities. Prior to segmentation, a preprocessing step was needed in which all ".tiff" image files are read into memory and stored in a 3-D matrix with 16-bit values and grayscale intensity values corresponding to the density of the features. The 3-D matrix values were down-converted to 8-bits to be compatible with most of Matlab's image-processing algorithms. To reduce memory load and computation time, the 3-D matrix was cropped in all dimensions to include minimal empty space surrounding the projectile. The threshold values for segmentation of the features were determined from random sampling of several projectiles. The threshold values given the image brightness of these CT scans are shown in the following table. Threshold values consistently segmented the desired components for nearly all of the (210) projectiles due to a significant difference in intensity values between the components, as they have a large enough difference in densities. However, it was found that on occasion the overall brightness of the entire volume was different enough that the component intensities would move into a neighboring threshold range, resulting in misclassification. To correct for these instances, a baseline intensity value was obtained from the Plexiglas plate on which the projectile stood, and the entire volume intensity was corrected by the offset from the standard intensity value of 35.

Table 8-bit grayscale threshold values used to segment various components

Component	8-bit grayscale voxel value
Empty space	$v \leq 35$
Silica filler	$35 < v \leq 49$
Steel jacket	$49 < v \leq 71$
Lead jacket and tungsten carbide core	$v > 71$

Three new 3-D binary matrices, one for each of the components, were created based upon the segmentation thresholds. A Logical 1 indicated a voxel intensity within the segmentation threshold, thus belonging to a particular component, and a Logical 0 indicates a voxel outside of the threshold. The volumes contained in these matrices for the outer steel jacket and the inner lead jacket and core were filled with Logical 1s such that there were no interior holes in the component shape so that the volume is solid and completely manifold.

2.2.2 Component Dimensioning via Circle Fitting

After segmenting binary volumes for each component, the second objective of the CT analysis algorithm was to fit circles to the outer parameter of each 2-dimensional (2-D) slice along the length of the axial symmetric projectile. Matlab's built-in function *imfindcircles* was used to locate and estimate the radii in pixels. This function uses a Circular Hough Transform (CHT)-based algorithm[1,2] and was operated using the "TwoStage" computation method as it proved to be more robust than the faster "PhaseCode" method. This function also requires as an input a range from which the radius to be fit is expected to be found. A narrow range improves the estimation speed and accuracy. However, the outer jacket shape and the inner jacket/core shapes taper in their radius as they approach the projectile tip. In addition, there tends to be a discontinuity at the end of the lead jacket as the radius suddenly decreases to the core tip radius. Therefore, an adaptable narrow range was provided to the algorithm by only considering potential radii that could fall between 90% and 110% of half of the average count of pixels (radius) along 2 lines of pixels that were obtained through the center of the slice, one in the x-direction and the other in the y-direction.

An example of the circle-fitting function is shown in Fig. 3 for a slice in the volume taken at 450 pixels in the z-direction from the base of the projectile. For the fit of the core volume, this is a location after the end of the lead jacket. The estimated radius for the outer jacket at this location is 96 pixels, and the core radius is estimated at 48 pixels. These circle fits are repeated along the entire length of the 3-D volume and result in a vector of radii for the core and the jacket as shown in Fig. 4 for Projectile 002. From this plot of the radii vectors some minor noise of a few pixels is seen along both profiles. This is likely due to slight changes in the grayscaling along the perimeter of the components that may flip several voxels in or out of the respective threshold range. It was observed in many of the component profiles that there is often a significant fitting error near the base of the projectile where the outer jacket is crimped under. This is an area where the grayscale intensities tend to fluctuate considerably and can fall outside of the threshold limits in a portion of the perimeter, which results in a region that is not completely

manifold, and from which the circular fit fails. The radii vectors can also be used to determine when the lead jacket begins at the base of the projectile—or begins higher up on the core—as is the case with Projectile 002 shown in Fig. 4.

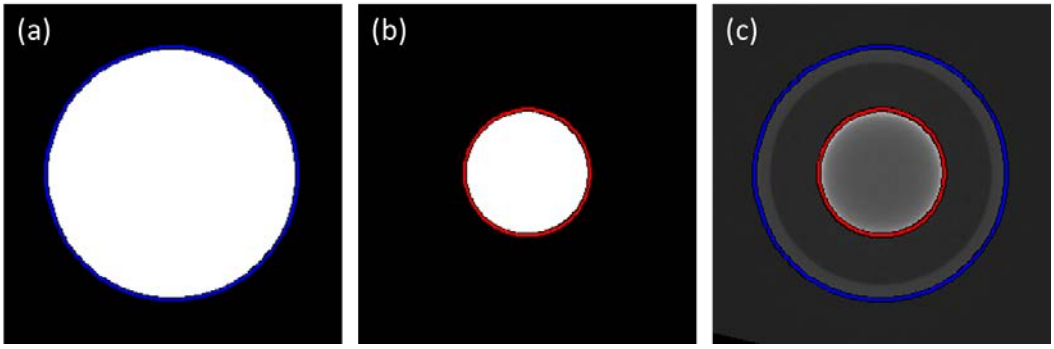

Fig. 3 Circle fit results (blue and red circles) performed on the perimeters of the slice at 450 pixels along the length of Projectile 002 (Fig. 2) of binary volume for the: a) jacket, and b) the tip of the core. c) Circle fits shown on the grayscale image from which the components were segmented.

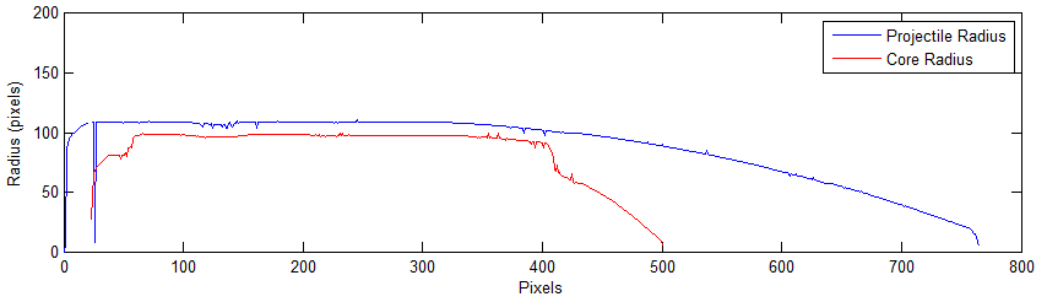

Fig. 4 Radii profiles for the outer steel jacket (blue) and internal lead jacket/core (red) of Projectile 002 (Fig. 1)

2.2.3 Powder Density Calculation

The density of the silica powder filler located after the core of the projectile is calculated for each slice as the density of pixels identified within the threshold range of the filler intensity (Logical 1 in the silica filler matrix) divided by the number of pixels interior to the outer jacket and exterior to the core. Therefore, if there is any empty space pixel between the filler that has an intensity value outside of the filler threshold range, then the numerator will decrease and the density will be reduced. It was found, however, that in practice the dynamic range in pixel intensities in the filler region was so narrow that empty space was not significantly detectable without severely reducing the filler threshold range, which resulted in wildly varying densities between projectiles. As such, the threshold range used was stable; however, it resulted in little contrast between the filler densities of different projectiles.

2.3 Batch Processing

The computational time of the CT analysis algorithm of a single projectile is on the order of 230 s on a single core of an Intel Xeon X5650 processor operating at 2.67 GHz. To batch process the (210) projectiles, a Matlab script was written to parallelize the processing by distributing the job to multiple cores, where up to 12 cores each analyzed a different projectile at the same time, thus reducing the overall computational time. The ".tiff" stacks for each projectile were saved in individually named folders on an external hard drive accessed over a FireWire connection. A total of 124 GB were required for the ".tiff" stacks. The output of the batch processing script were Matlab cell arrays of the outer jacket radii vectors, the inner jacket/core radii vectors, and the powder density vectors for each projectile.

3. Results

The goals of characterizing the structures of (210) projectiles were to numerically quantify the component properties (i.e., shape, position) of each projectile, understand manufacturing variability, and to obtain a subgroup of the most similar for later ballistic testing, while omitting outliers. These goals can be obtained by comparing the structures of the projectiles to each other using a metric of similarity. Then, projectiles that are the most similar can be grouped together and those least similar can be treated as outliers.

Before comparing one projectile to another, the profile vectors must be registered to each other such that the base and the tip are in an as close as possible z-position with each other. This is needed because often the CT scan position starts at different locations in the z-direction, thus shifting the z-position of the projectile. A cross-correlation algorithm built into Matlab (*xcorr*) was used to compare the outer jacket radii profile vector with a standard jacket radii profile vector to determine how far the unknown vector lagged the standard. The unknown projectile's position in the z-axis was then shifted to best align with the standard's position. In so doing, all (210) projectiles were registered to the position of a standard according to the profile of their outer jacket. After registration, all volumes should overlap in space and any deviation in their profile radii or position of jacket/cores can be directly comparable as best as possible.

The result of the registration and image analysis for the projectile population is shown in Fig. 5, where the average profiles for the outer steel jacket and the inner lead jacket/core are plotted along with the one standard deviation.

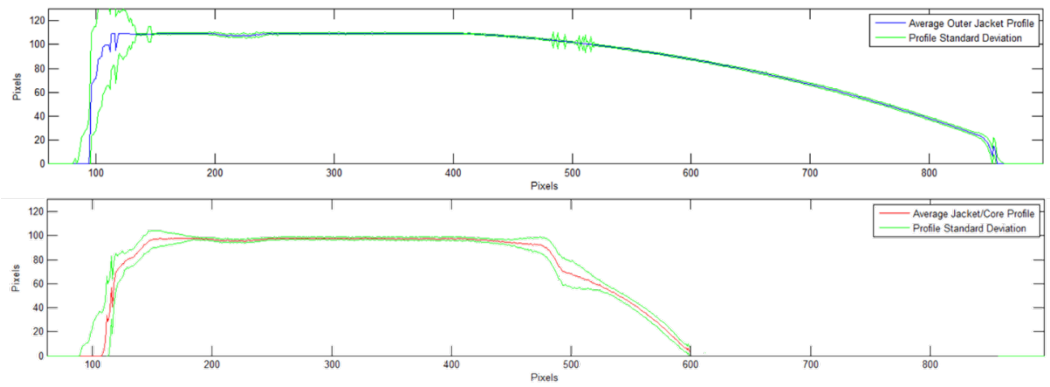

Fig. 5 Average profiles for the outer jacket (top) and the inner jacket/core (bottom). Lines indicating standard deviation of the profile population are shown with green lines.

The greatest dissimilarity between the outer jackets of the projectiles occurs near the base where the jacket is crimped under, the result of a large amount of circle fitting error (possibly due to beam hardening and X-ray scattering). Fitting error is also attributed to the large standard deviation in the outer jacket profile around the 500 pixel mark. The largest real differences between the projectile outer jackets is seen at the crimp location near 225 pixels, as well as an increasing difference with length in the cone region of the projectile. Compared to the outer jacket, the inner lead jacket and tungsten carbide core profiles show a much larger disparity in the population. While the diameter of the lead jacket is consistent, the location of the jacket along the length varies. There is also a large standard deviation in the core's cone region, which could be associated with either core shape and/or the position of the core.

A root-mean-square-error (RMSE) calculation, see Eq. 1, was used to calculate the similarity, or residuals, of the radii profiles between 2 projectiles. This calculation will tend towards zero as the profiles become more identical and differences are amplified. Therefore, it is important that the profiles are registered according to a common start and end point so that 2 nearly identical profiles are not considered dissimilar simply because of a shifted position in the z-axis. It was found that there was occasional, nonreal image-analysis/circle-fitting error within the first 150 pixels of the outer jacket radii profiles and the first 130 pixels of the jacket/core radii profiles that includes empty space and where the outer jacket was rolled under, which was ignored from the RMSE calculation. In addition, a region between 480 and 525 pixels in the outer jacket radii profile was ignored as it tended to have analysis/fitting noise at the discontinuity when the lead jacket stops on the core.

$$RMSE = \sqrt{\frac{\sum_{z=1}^{n}(p_{1z} - p_{2z})^2}{n}} \quad (1)$$

Eq. 1: RMSE calculation used to calculate the similarity of radii profiles between 2 projectiles (a pair).

The RMSE equation was used to calculate the profile error between every possible pairing of projectiles. These dissimilarity values were normalized by the maximum pair difference value, and are plotted in Figs. 6 and 7, respectively, for the outer jacket and the inner jacket/core. These results show that if a radii profile for a projectile is dissimilar to some projectiles, then it tends to be dissimilar to most projectiles as indicated by high-value striping, or lines spanning the entire plot, meaning there is high-dissimilarity intersection with all tiles (e.g., Projectiles 33 and 52). This striping indicates that the features that cause a projectile to be dissimilar tend to be unique.

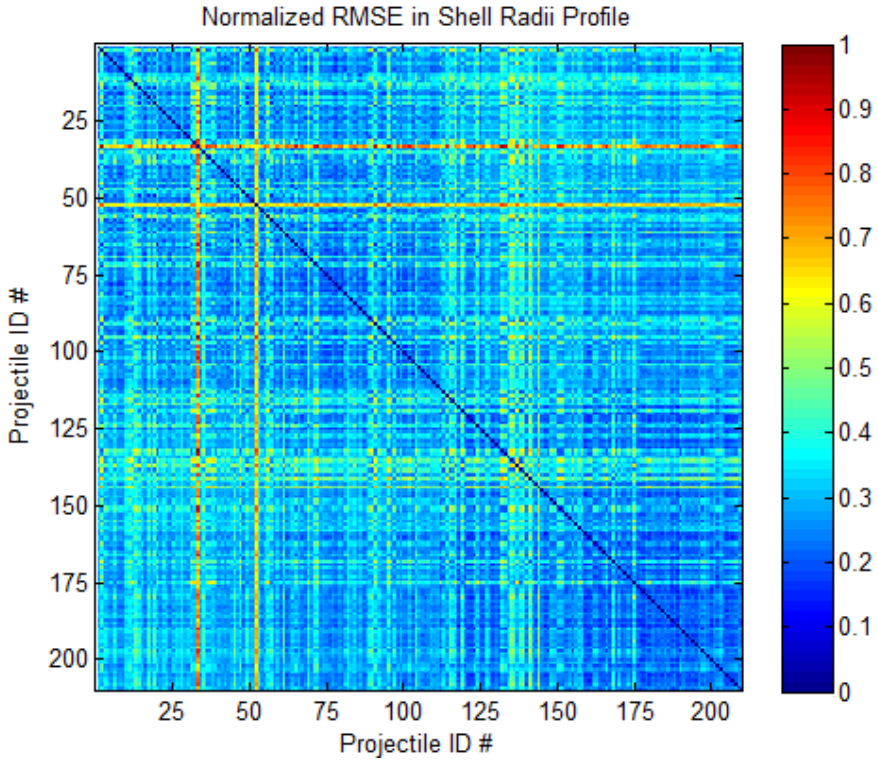

Fig. 6 RMSE comparison between projectiles in outer jacket (shell) radii profiles normalized by the maximum difference value. A value of zero represents identical profiles.

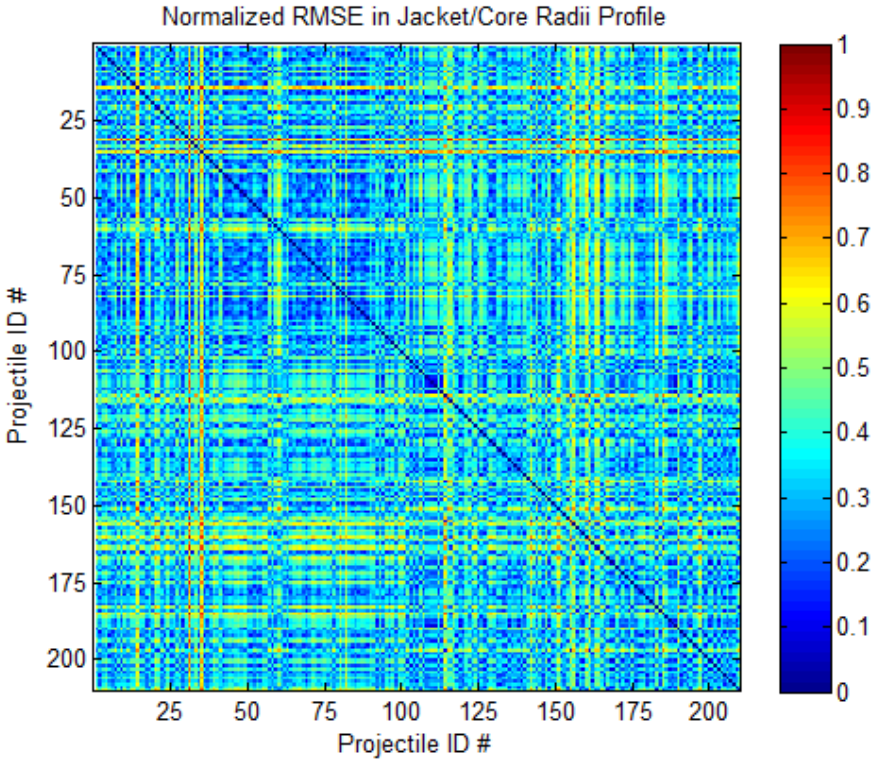

Fig. 7 RMSE comparison between projectiles in jacket/core radii profiles normalized by the maximum difference value. A value of zero represents identical profiles.

To sort these projectiles from most similar to least similar the following algorithm was used on the sum of the RMSE matrices plotted in Figs. 6 and 7. Because these matrices are normalized they have equal weighting so that when summed together the highest possible dissimilarity value would be 2.

1) Find the projectile that is most similar to all others (lowest total RMSE when paired with others) and add to the list.

2) Add the projectile to the list that has the most similarity with projectile(s) already in the list.

3) Repeat Step 2 until all projectiles have been added.

This algorithm was specifically used because it does not simply sort the projectiles from most similar to least similar, but instead will first form a *group* of the most similar projectiles and add on projectiles of increasing dissimilarity to projectiles in that group. For example, if the population was bimodal according to a feature (e.g., lead jacket position), then this algorithm would begin by grouping and then sorting the feature that had the largest subpopulation and then would eventually add in projectiles from the second subpopulation in the order that they are similar to the first group. This is in contrast to a direct sort based upon the lowest total RMSE

values for each projectile, which could alternate between the 2 populations by a simple ranking of most similar to least similar. Therefore, the algorithm will sort projectiles within groups of decreasing size that could have projectiles with features that are significantly different than the features of projectiles in the other groups. The result of sorting the combined RMSE matrices for the outer jacket and the inner jacket/core are shown in Fig. 8, where the projectiles that are the most similar to each other are grouped in the upper left of the plot. The most similar projectiles have the lowest average combined RMSE in their radii profiles to the other projectiles.

This sorted matrix also reveals groups of more similar projectiles, which are visible as boxes of darker blue (lower combined RMSE), that follow the identity diagonal. The radii profiles of the 15 most similar projectiles and the 15 least similar projectiles according to the similar RMSE sorting algorithm are shown in Fig. 9. It is apparent that the most similar projectiles have commonality in their outer jacket shape, core tip shape, and most notably, the inner lead jacket position. This is in contrast to the 15 least similar radii profiles in which there is greater deviation in the outer jacket shape (i.e., thickness and tip shape), the core position, and especially, the lead jacket position. While the core and jacket appear to move considerably with the least similar projectiles, the overall position of the projectile in the z-direction is fairly consistent due to the use of the cross-correlation registration step, which allows the projectiles to be directly comparable to one another in the z-direction. The outer jacket crimp location is consistent around 225 pixels in the z-direction for both the most and least similar profiles, even though the core and jacket locations might vary.

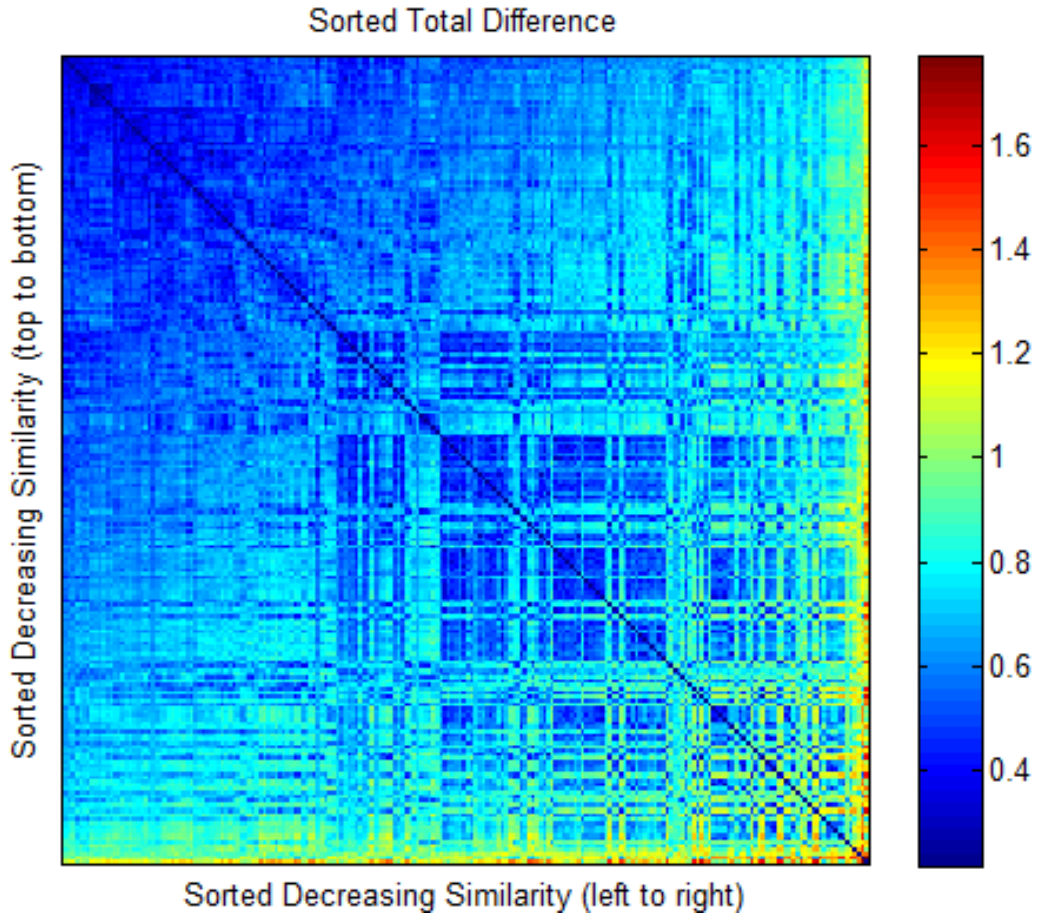

Fig. 8 Combined normalized RMSE between the outer jackets and the inner jackets/cores of projectiles sorted from most to least similar

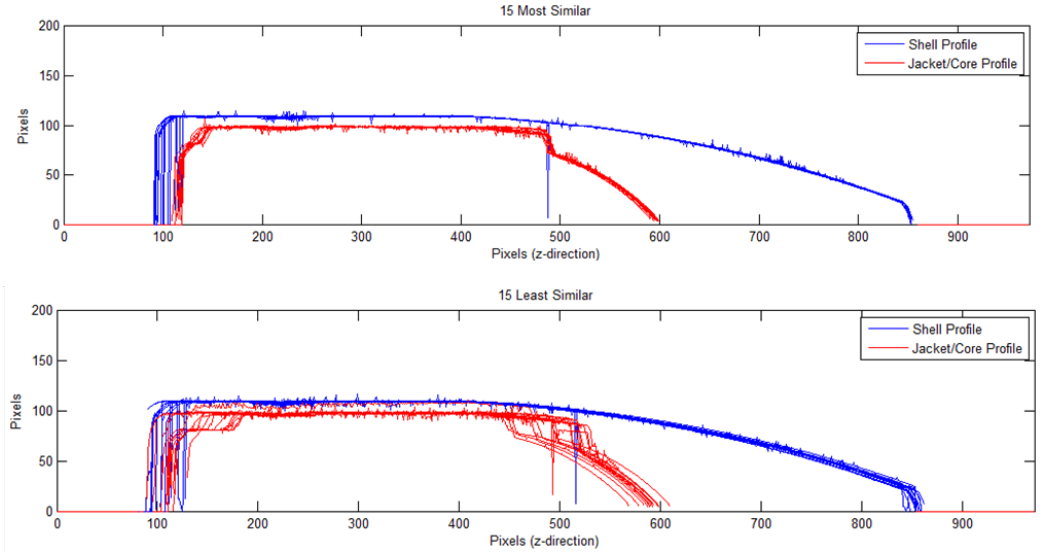

Fig. 9 Radii profiles for the most similar projectiles (top) and the least similar projectiles (bottom) according to the similarity sorting algorithm

Clustering

It appears that the greatest variability exists in the jacket/core component of the projectiles, with the potential for the lead jacket to be positioned at various positions along the core as well as variability in the core's position in the z-direction. According to the sorting algorithm results shown in Fig. 8 there are several groups of projectiles with a common feature. To further understand the different groups of features that may be present in the jacket/core, a clustering method was applied to the jacket/core radii profiles. K-means clustering of the profiles into 15 clusters was performed. After clustering, the distance in p-dimensional space (each pixel position in the z-direction is a separate p-dimension) between each cluster center was found. Next, the mean distance between each cluster and their second closest neighbor was set as the cutoff criteria for placing an edge between clusters. Therefore, 2 clusters are considered neighbors and connected by an edge if the distance between them is less than or equal to the cutoff criteria. This results in an adjacency matrix with some outlying clusters not connected to any other cluster due to distance. It also results in some close, but distinct, clusters having more than 2 neighbors. A Fruchterman-Reingold[3] algorithm was then applied to the adjacency matrix to generate a force-directed graph, resulting in a geometrically sprawling representation of the data. These results are shown in Figs. 10 and 11, respectively, where plots of the profiles contained within each cluster are overlaid to aid in understanding the reason for clustering.

The results show a giant structure that links similar profiles together with several distant surrounding clusters that could be considered as outliers. The profiles contained in each cluster in the giant structure are fairly consistent between themselves. The largest cluster in the giant structure, which has 32 profiles and 5 edges connecting to nearest clusters, appears to be the most average in terms of inner jacket and core positions as well as inner jacket length. It also contains profiles that look most representative of the 15 most similar profiles shown in Fig. 9. This cluster connects to neighboring clusters where the core tip ends closest to the 600-pixel mark in the z-direction. However, 2 of those neighboring clusters have jackets that start further up the core in the z-direction, whereas the other 3 have jackets that start near the bottom of the core and projectile. The most noticeable aspect of the remaining clusters, which are not connected directly to the largest cluster, are jackets that start further up on the core. Additionally, these profiles have core tips that stop short of the 600-pixel mark. This appears to be caused by either the core starting at a lower z-direction position—as in the case of the 9 profile cluster with only one edge—or the core appears to be shorter in total length—as in the case of the cluster with 7 profiles and 2 edges.

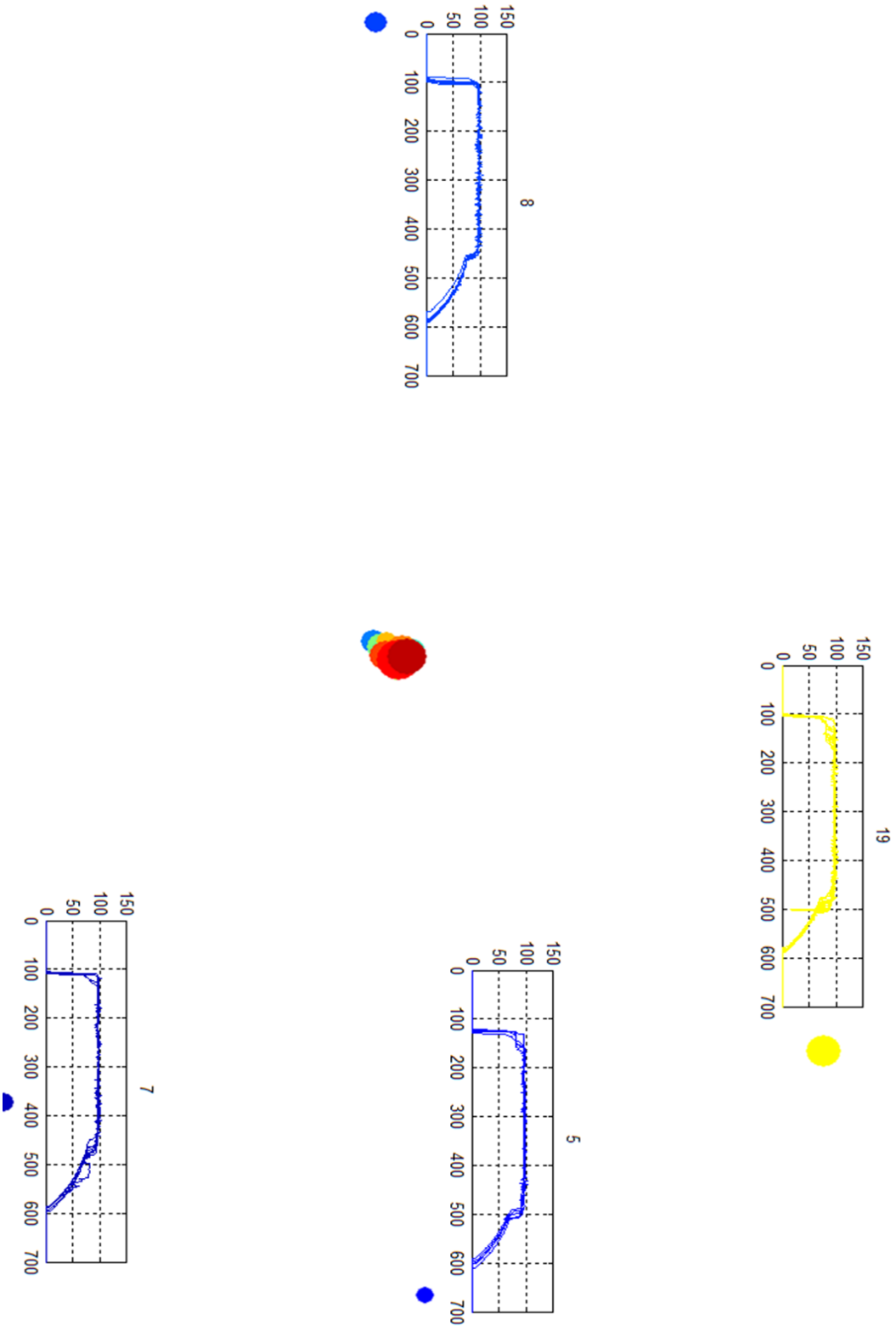

Fig. 10 Graphical structure of 15 clusters of the jacket/core radii profiles with plots of the profiles contained within each cluster. The size of the dot and the number above the plots indicate the cluster size. Clusters in the center of the plot are from the giant structure shown in Fig. 11.

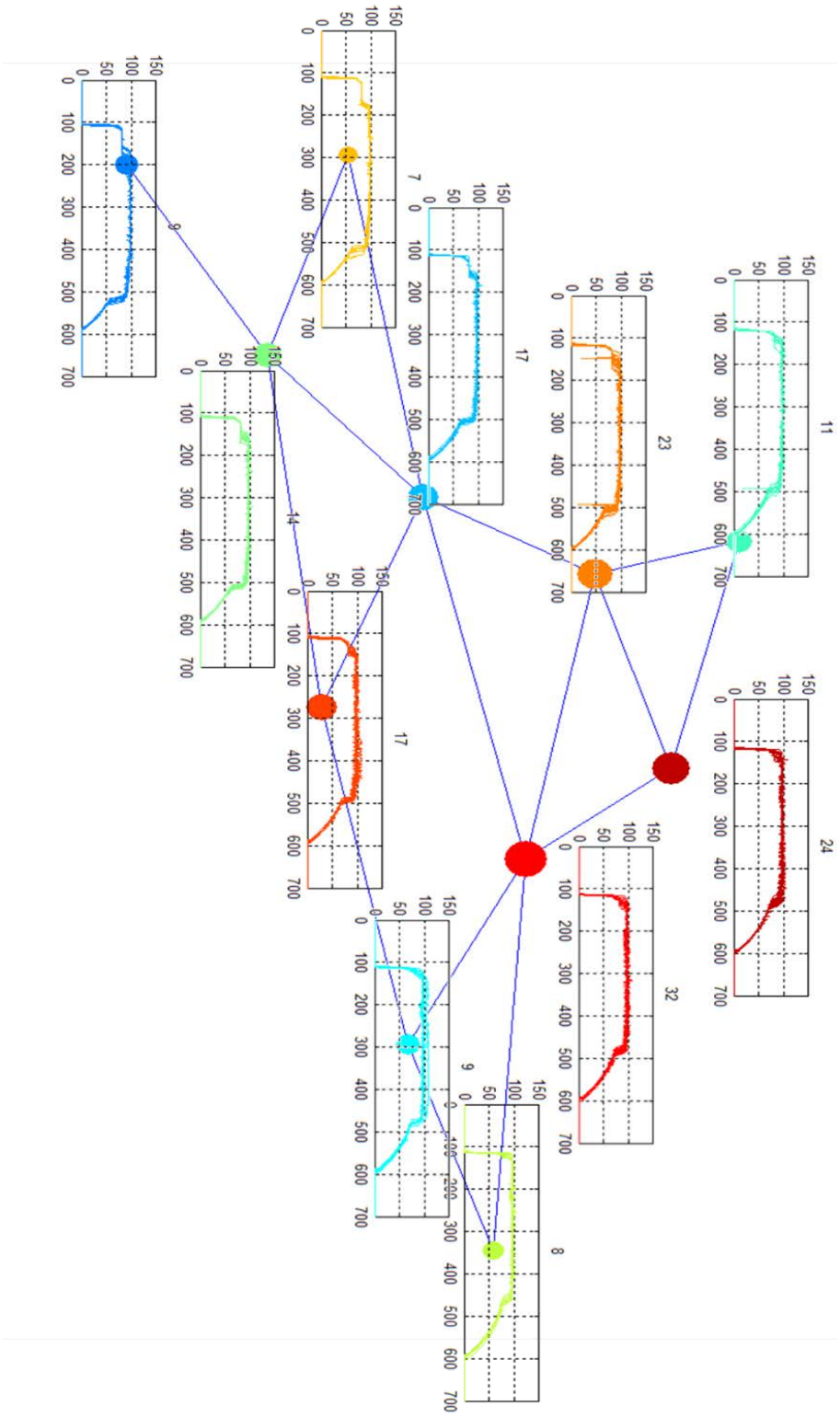

Fig. 11 Giant structure formed by clustering of the jacket/core radii profiles with plots of the profiles contained within each cluster. The size of the dot and the number above the plots indicate the cluster size. Lines indicate nearest or related clusters.

4. Summary and Conclusions: Implications for the Use of Cartridge Projectiles in Armor Evaluation

This report details an algorithm for batch processing CT image data of BS41 surrogate projectiles to numerically quantify projectile component properties, which enables the determination of manufacturing variability and the ability to rank projectiles by feature similarity. The algorithm uses Matlab's image-processing toolbox functions to fit circles to the segmented features found within the projectile to obtain an axial-symmetric radii profile, which can be used to compare projectiles. Then, by sorting projectiles by feature similarity, a most-similar group was formed that had nearly identical shape and positioning of components. Most variability was found in the shape and location of the inner lead jacket and WC-Co core. Graphical clustering of the projectiles by commonality in their component features provides insights into the uniqueness of features and enables rapid understanding of projectile variability through a visual map of the possible component arrangements.

The use of cartridge projectiles can be a source of measurement uncertainty in the ballistic evaluation of armor if there is variability in their construction from one projectile to the next. The analysis of the (210) projectiles studied as part of this work shows that variability does exist, especially with the inner jacket/core properties, but the role the observed variability has on the projectile/armor interaction is unknown. However, by prescreening projectiles using this CT method, the effects of variability can be minimized. The grouping algorithm could be used to group projectiles according to similarity. Subsequent graphical cluster analysis can be used to find the most similar groups, from which a population of the most similar projectiles can be selected for use as test projectiles. Then, to help account for variability in the measurement of a projectile/target interaction, the method described can be used to obtain an RMSE value between test projectiles and a standard projectile. This would provide a scalar numerical value that summarizes how different a projectile is from the standard, and could provide an input to the armor performance model, along with the other test conditions such as velocity, pitch, and yaw.

5. References

1. Atherton TJ, Kerbyson DJ. Size invariant circle detection. Image and Vision Computing. 1999;17(11):795–803.
2. Yuen H, Princen J, Illingworth J, Kittler J. Comparative study of Hough transform methods for circle finding. Image and Vision Computing. 1990;8(1):71–77.
3. Traud AL, Frost C, Mucha PJ, Porter MA. Visualization of communities in networks. Chaos. 2009;19(4):041104.

List of Symbols, Abbreviations, and Acronyms

2-D	2-dimensional
3-D	3-dimensional
ARL	US Army Research Laboratory
CHT	Circular Hough Transform
CT	computed tomography
RMSE	root-mean-square-error
WC-Co	tungsten carbide cobalt

1 (PDF) DEFENSE TECHNICAL INFORMATION CTR DTIC OCA

2 (PDF) DIRECTOR US ARMY RESEARCH LAB RDRL CIO LL IMAL HRA MAIL & RECORDS MGMT

1 (PDF) GOVT PRINTG OFC A MALHOTRA

1 (PDF) DIR USARL RDRL WMM E M GOLT

INTENTIONALLY LEFT BLANK.